ISSN 0020-1685, Inorganic Materials, 2014, Vol. 50, No. 12, pp. 1185–1190. © Pleiades Publishing, Ltd., 2014.
Original Russian Text © A.I. Nepomnyshchikh, R.V. Presnyakov, P.V. Antonov, V.S. Berdnikov, 2014, published in Neorganicheskie Materialy, 2014, Vol. 50, No. 12, pp. 1281–1286.

Effect of Crucible Rotation Rate on the Growth and Macrostructure of Multicrystalline Silicon

A. I. Nepomnyshchikh[a], R. V. Presnyakov[a], P. V. Antonov[b], and V. S. Berdnikov[b]

[a] *Vinogradov Institute of Geochemistry, Siberian Branch, Russian Academy of Sciences, ul. Favorskogo 1A, Irkutsk, 664033 Russia*

[b] *Kutateladze Institute of Thermal Physics, Siberian Branch, Russian Academy of Sciences, pr. Akademika Lavrent'eva 1, Novosibirsk, 630090 Russia*

e-mail: ropr@igc.irk.ru

Received February 7, 2014

Abstract—This paper examines the influence of uniform rotation of the crucible–melt–crystal system in a flat-bottom Bridgman geometry on the columnar silicon structure formed by a flat solidification front. We analyze the key features of heat exchange via natural convection using numerical simulation of experimental conditions of the growth of multicrystalline silicon from high-purity metallurgical-grade silicon.

DOI: 10.1134/S0020168514110119

INTRODUCTION

Fundamental issues in alternative power generation technologies include the development of physical principles of the energy-efficient preparation of solar-grade silicon from metallurgical-grade silicon produced by the carbothermic process [1]. The basic material for solar power conversion technologies is multicrystalline silicon. An important issue in the growth of this material is the interrelationship between the particular character of heat and mass transport and the forming columnar structure. FCC crystals are known to contain general and special boundaries [2]. The general boundaries form well-seen parent grains that have a nearly polyhedral shape when observed in a cross section parallel to the solidification front. The parent grains contain special boundaries due to twinning on the {111} planes. This configuration requires less energy than the formation of general boundaries, and the corresponding microstructure of silicon has a negligible effect on carrier transport [3].

THEORETICAL ANALYSIS

The starting material for the growth of silicon ingots with a columnar structure was 99.76 at % pure, which was ensured by the quality of reductants and silica in the carbothermic process [4]. Silicon solidification was accompanied by the rejection of the impurities indicated in the table to the melt.

During crystal growth, constitutional supercooling develops at the instant when the temperature gradient in the boundary layer becomes lower than that along the tangent to the liquidus line. Therefore, the minimum ratio of the temperature gradient to the crystal growth rate necessary for creating a stably smooth interface is given by

$$\frac{1}{V}\frac{\partial T}{\partial z} = \frac{\partial T_L}{\partial C_L}\frac{C_0(1-k_0)}{k_0 D}, \quad (1)$$

where k is the equilibrium impurity distribution coefficient, D is the impurity diffusion coefficient in the melt, V is the crystal growth rate, $\partial T/\partial z$ is the temperature gradient in the boundary layer along the normal

Impurity concentrations in the starting silicon, slope of the liquidus line, and decrease in liquidus temperature

Element	C_0, ppmw	$\partial T_L/\partial C_L$, K/ppmw	$\Delta T = C_0\,\partial T_L/\partial C_L$, K
B	12	9.1×10^{-4}	0.0109
P	30	3.1×10^{-4}	0.0093
Al	175	5.1×10^{-4}	0.0892
Cu	8	1.9×10^{-4}	0.0015
Mg	11	7.4×10^{-4}	0.0081
Ca	27	5.4×10^{-4}	0.0146
Fe	850	2.4×10^{-4}	0.2040
V	60	2.8×10^{-4}	0.0128
Co	70	2.4×10^{-4}	0.0168
Ti	70	2.0×10^{-4}	0.0140
Mn	35	3.1×10^{-4}	0.0108
Ni	37	2.8×10^{-4}	0.0104
Cr	3	2.1×10^{-4}	0.0006
Zr	30	1.7×10^{-4}	0.0051

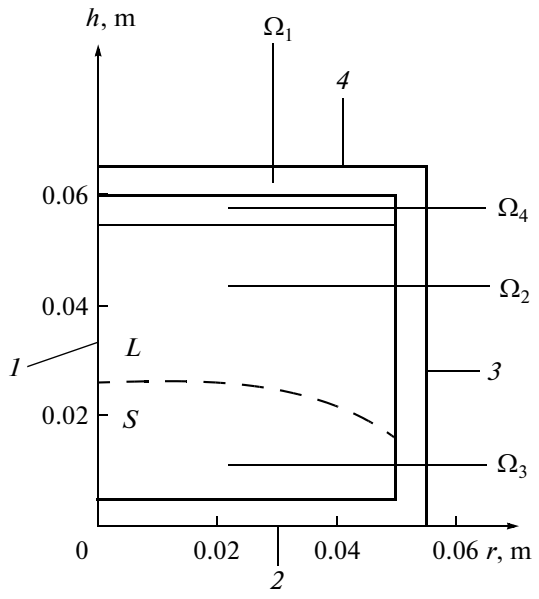

Fig. 1. Schematic representation of the two-dimensional simulation region (r is the radial coordinate and h is the height): Ω_1, graphite crucible; Ω_2, liquid silicon (L); Ω_3, solid silicon (S); Ω_4, vacuum layer; boundaries of the region: (*1*) crucible rotation axis, (*2*) outer bottom of the crucible, (*3*) outer lateral wall of the crucible, (*4*) surface of the lid of the crucible.

to the interface (T is the absolute temperature and z is a coordinate), $\partial T_L/\partial C_L$ is the slope of the liquidus line in the phase diagram (T_L is the liquidus temperature and C_L is the corresponding impurity concentration), and C_0 is the impurity concentration in the melt beyond the boundary layer [5]. Assuming that the influence of each impurity on the liquidus temperature is linear and independent of the other impurities and that their mutual influence on diffusion processes can be neglected, we find that, for a multicomponent composition, the right-hand side of Eq. (1) is the sum over individual impurities.

EXPERIMENTAL

In the Bridgman growth of multicrystalline silicon, a 2-mm-thick glassy carbon crucible tightly embedded in a 8-mm-thick graphite support was held at constant temperature in the top zone of a resistive heater during silicon melting and melt homogenization. Next, the crucible was slowly lowered into the gradient zone. This led to melt cooling from below. As a result, the geometric selection of nuclei occurred on the flat bottom of the crucible at some instant in time, followed by the formation of a columnar structure.

The composition of the starting metallurgical-grade silicon corresponds to an overall decrease in liquidus temperature by 0.4 K for all of the elements present. During growth, this parameter will increase with an increase in the fraction of melt solidified. We carried out preliminary laboratory experiments aimed at finding the maximum permissible travel rate of the crucible–melt–crystal system in a given temperature gradient that will ensure stability of the crystal–melt interface using Eq. (1) as a criterion [6]. Depending on the temperature gradient, the crucible lowering rate was either 5 (gradient of 5 K/cm) or 15 mm/h (gradient of 15 K/cm).

The macrostructure of the ingot was examined visually after lapping the surface of a longitudinal section with 28-μm corundum micropowder, followed by etching in a KOH solution (10%).

In numerical simulation of the hydrodynamics and associated heat exchange under experimentally determined growth conditions, a working crucible in the shape of a truncated cone was represented by an MPG-6 graphite cylinder with a 10-mm-thick wall and bottom, containing the same volume of the melt. Calculation for the region represented in Fig. 1 was based on solving the Navier–Stokes energy and continuity equations with the temperature, current, circumferential speed, and vortex as variables, in combination with boundary conditions. The thermophysical properties of the materials were taken constant at the average temperature. The difference in density between solid and liquid silicon was neglected. To solve equations for natural convection and the heat equation, we used the finite element method. In Fig. 1, solid and liquid phases with different thermophysical properties are separated by the silicon melting isotherm in the approximation of normal growth of an atomically rough surface [7].

RESULTS AND DISCUSSION

The impurity distribution over a silicon-based ingot of 99.76 at % purity depends significantly on the solidification rate. At a ratio of the temperature gradient to the crucible translation rate below a critical level (3.6×10^8 K s/m^2), interface breakdown occurs, leading to the formation of cellular/dendritic structures as a result of constitutional supercooling [6]. Because of this, the ingot section surface was chemically etched in order to determine the position of the solidification front at the instant when external heating was switched off (Fig. 2). Because of the high heat capacity of the melt, this procedure is inappropriate in the case of n-type silicon because columnar growth then continues in the central part of the crucible and begins from the lateral wall (Fig. 2b). Microstructural analysis showed that the rate of crucible rotation, used to level off the external thermal field, influenced the columnar structure of the ingots (Fig. 3), without distorting the planar shape of the solidification front (Figs. 2a, 3b).

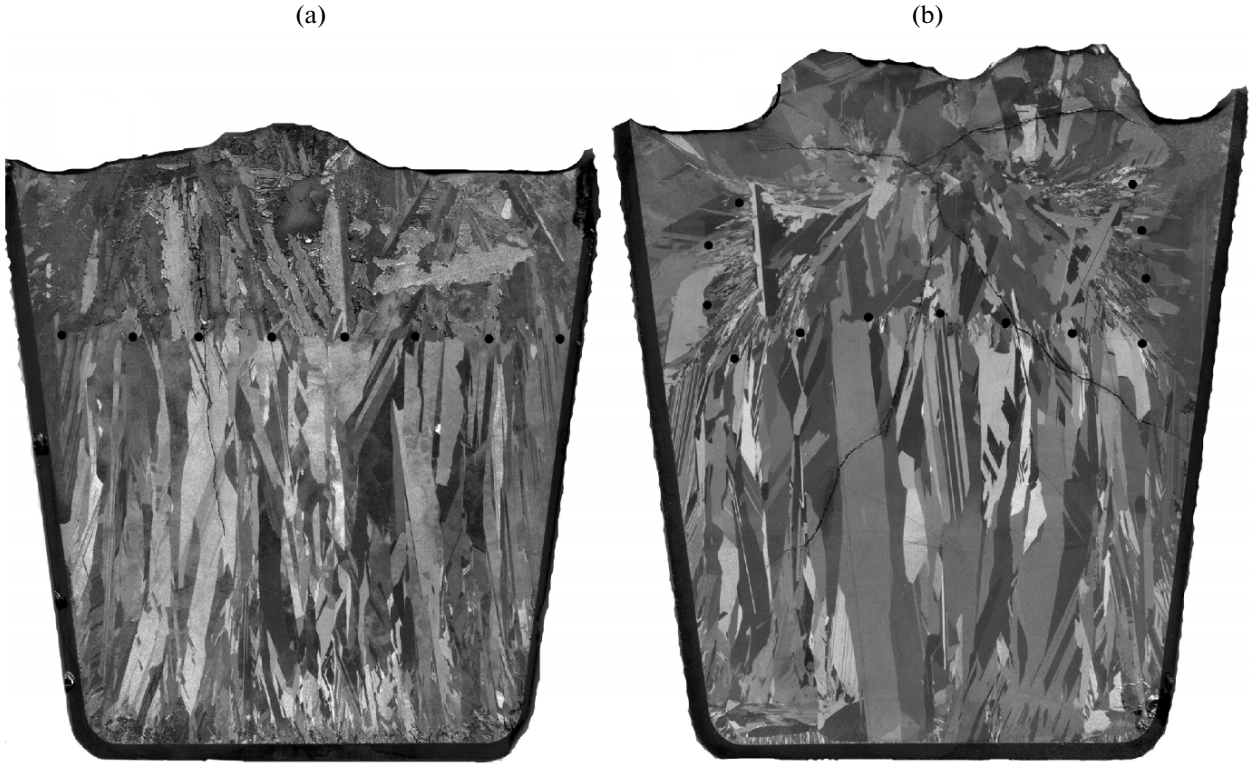

Fig. 2. Boundaries of the columnar growth and rapid freezing regions in ingots grown from (a) 99.76 at % pure silicon with crucible rotation at 6 rpm and (b) from 99.99999 at % pure silicon without crucible rotation.

Figure 3 demonstrates that the size of the parent grains with accompanying plane-parallel twinning increases as the crucible rotation rate decreases from 1 to 0.1 rpm. To assess the effect of uniform crucible rotation on the associated heat exchange in the crucible–melt–crystal system, we constructed temperature fields at one-quarter and half of the melt solidified (Fig. 4).

Since the thermal conductivity of the crucible exceeds that of molten silicon, the heat removal from the melt through the crystal is accompanied by a downward heat flow from the superheated, upper part of the crucible through the lateral wall. The melt superheating regions near the crucible lead to a torus-like flow, with an ascending flow near the lateral wall and a descending flow in the central part [7]. At crucible rotation rates in the range 0–1 rpm, the amplitude of the convective flow varies insignificantly, but its structure experiences marked changes. Because of the viscous friction, the descending flow creates one or several recirculation zones near the crucible axis, with a lower flow speed. Owing to the high thermal conductivity of the melt, the weak flow near the axis cannot influence the temperature field and cannot prevent the directional melt cooling through the crystal. Because of this, the isotherms become again convex near the axis. Without crucible rotation, the isotherms near the axis are concave because the descending convective flow prevents growth in the central part.

As a result of the described processes, increasing the crucible rotation rate from 0 to 1 rpm reduces the solidification temperature near the axis. At the point where the rotation axis of the system intersects the dashed line representing the real solidification front, the decrease in solidification temperature is about 1 K at one-quarter of the melt solidified and more than 3 K at half of the silicon solidified. These values are comparable to the initial supercooling (~4 K) during layer-by-layer growth of the {111} faces, which have the lowest surface energy in silicon [8].

The associated heat exchange model characterizes normal growth in which any supercooling at the interface is a driving force of the kinetic process ($V \sim \Delta T$). In effect, there are the following components of the total supercooling: ΔT_R, a correction related to the excess surface energy; ΔT_C, constitutional supercooling; and ΔT_L, a correction related to latent heat removal. The removal of the heat of crystallization into the solid phase was taken into account by introducing an effective heat capacity into the heat equation [7]. At one-quarter and half of the melt solidified, $\Delta T_C \approx 0.5$ K and $\Delta T_C \approx 0.8$ K, respectively. At the same time, the ΔT_C correction can be left out of consideration, because Eq. (1) can be reached in experiments.

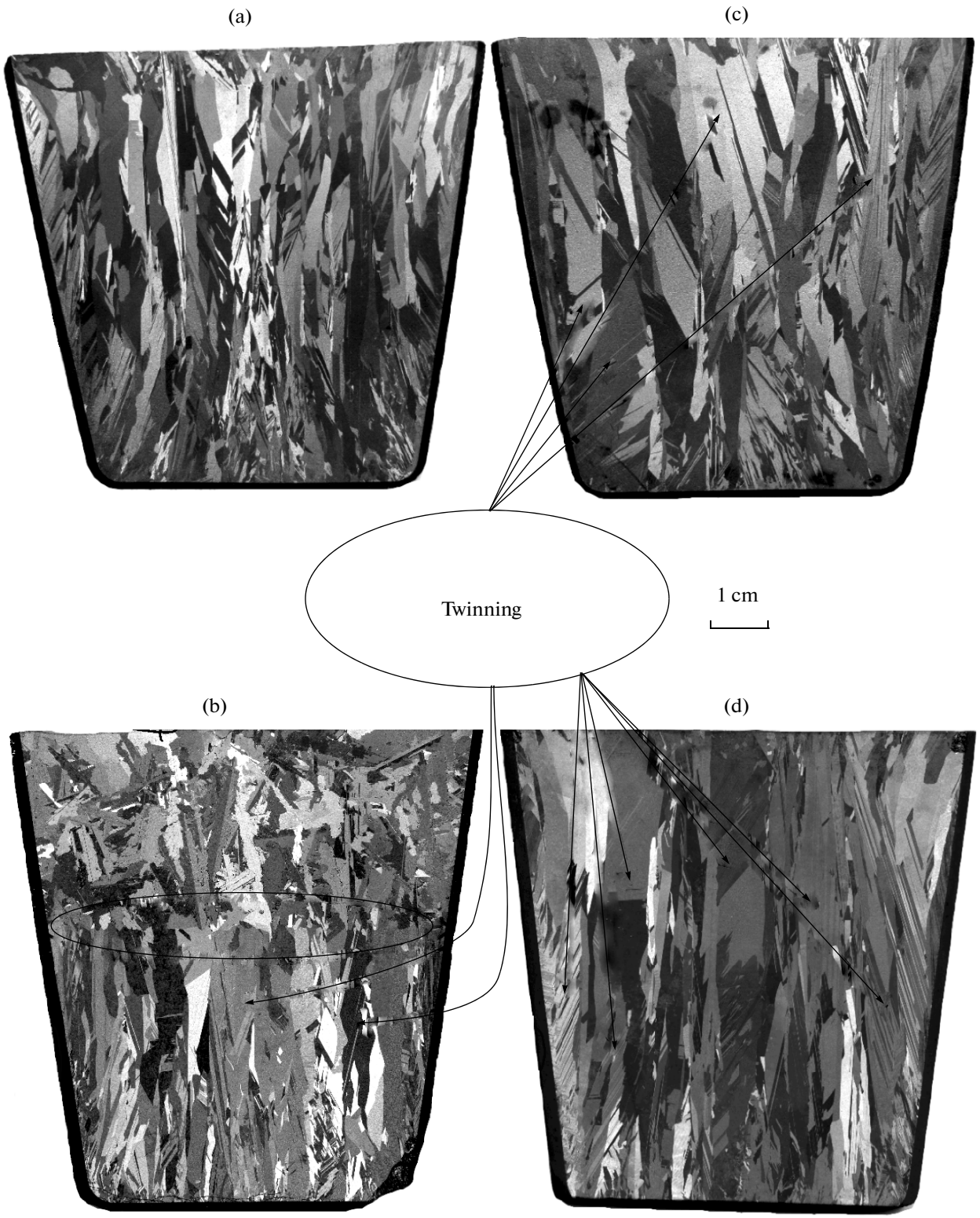

Fig. 3. Twinning in the structure of longitudinal sections of the ingots grown with crucible rotation: (a) 1 rpm, (b) 0.65 rpm (the boundary between the columnar and dendritic structures on the section indicates the shape of the solidification front), (c) 0.5 rpm, (d) 0.1 rpm.

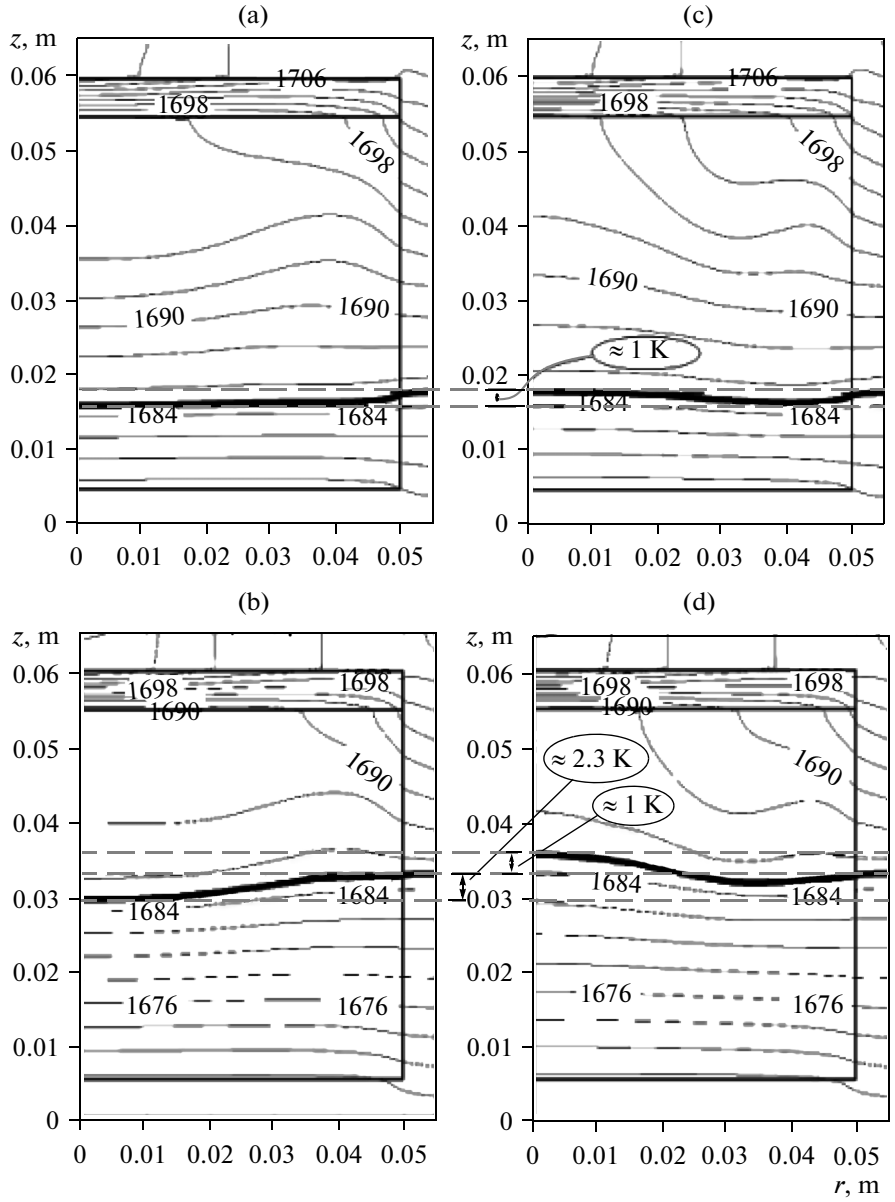

Fig. 4. Temperature fields in the crucible–melt–crystal system at one-quarter and half of the melt solidified: (a, b) without rotation, (c, d) crucible rotation at 1 rpm. The numbers in the ellipses indicate the temperature difference between the outer crucible wall and the crucible rotation axis at a given height.

Because of this, the forming macrostructure depends on how the surface energy of the growing crystal is minimized. In particular, the interface may be formed by the {111} planes in the form of reentrant angles, on which parallel twins may appear [8, 9]. In such a case, supercooling depends on the crystallographic orientation of the parent grains and reaches 70–80% of the initial one for the {111} value at a given growth rate [10]. The decrease in the temperature of the growing surface in the central part with increasing crucible rotation rate is due to the excess surface energy, which goes into the formation of general grain boundaries.

CONCLUSIONS

We have studied the macrostructure of multicrystalline silicon and analyzed silicon growth conditions on a flat solidification front under natural convection conditions. One way of influencing natural convection is by rotating the crucible and melt. In the case of crucible rotation, its angular speed is determined by the necessity of axisymmetric multicrystalline silicon growth in a nonuniform temperature field, which takes place almost always under real conditions. The bending of the isotherms in the axial region of the melt–crystal interface is caused by the partial suppression of natural convection. For the formation of large

parent grains (~1 cm in size), accompanied by plane-parallel twinning, columnar silicon growth is necessary, with planar isotherms near the phase transition.

REFERENCES

1. Gribov, B.G. and Zinov'ev, K.V., Preparation of high-purity silicon for solar cells, *Inorg. Mater.*, 2003, vol. 39, no. 7, pp. 653–662.
2. Konovalova, E.V., Koneva, N.A., Perevalova, O.B., and Kozlov, E.V., Structure of the grain-boundary ensemble in single-phase fcc polycrystals, *Fiz. Mezomekh.*, 2000, vol. 3, no. 3, pp. 15–22.
3. Wang, H.Y., Usami, N., Fujiwara, K., Kutsukake, K., and Nakajima, K., Microstructures of Si multicrystals and their impact on minority carrier diffusion length, *Acta Mater.*, 2009, vol. 57, no. 11, pp. 3268–3276.
4. Nepomnyashchikh, A.I., Eremin, V.P., Krasin, B.A., Vasil'eva, I.E., Eliseev, I.A., Zolotaiko, A.V., Popov, S.I., and Sinitskii, V.V., Multicrystalline silicon for solar power conversion, *Izv. Vyssh. Uchebn. Zaved., Mater. Elektron. Tekh.*, 2002, vol. 4, no. 2, pp. 16–24.
5. Mullins, W.W. and Sekerka, R.F., Stability of a planar interface during solidification of a dilute binary alloy, *J. Appl. Phys.*, 1964, vol. 35, no. 2, pp. 444–451.
6. Nepomnyashchikh, A.I., Presnyakov, R.V., Eliseev, I.A., and Sokol'nikova, Yu.V., Specific features of multicrystalline silicon growth from high-purity commercial silicon, *Tech. Phys. Lett.*, 2011, vol. 37, no. 8, pp. 739–742.
7. Antonov, P.V. and Berdnikov, V.S., Effect of heat exchange conditions on the shape of the solidification front and silicon growth rate in the Bridgman–Stockbarger process, *Prikl. Mekh. Tekh. Fiz.*, 2012, vol. 53, no. 6, pp. 65–77.
8. Fujiwara, K., Obinata, Y., Ujihara, T., Usami, N., Sazaki, G., and Nakajima, K., Grain growth behaviors of polycrystalline silicon during melt growth processes, *J. Cryst. Growth*, 2004, vol. 266, no. 4, pp. 441–448.
9. Fujiwara, K., Maeda, K., Usami, N., Sazaki, G., Nose, Y., and Nakajima, K., Formation mechanism of parallel twins related to Si-facetted dendrite growth, *Scr. Mater.*, 2007, vol. 57, no. 2, pp. 81–84.
10. Miyahara, H., Nara, S., Okugawa, M., and Ogi, K., Effect of twin growth on unidirectional solidification control of multicrystal silicon for solar cells, *Mater. Trans.*, 2005, vol. 46, no. 5, pp. 935–943.

Translated by O. Tsarev